

Time Exposure Acoustics

Stephen J. Norton and I. J. Won

Abstract—An analysis of a passive seismic method for subsurface imaging is presented, in which ambient seismic noise is employed as the source of illumination of underground scatterers. The imaging algorithm can incorporate new data into the image in a recursive fashion, which causes image background noise to diminish over time. Under the assumption of spatially-incoherent ambient noise, an analytical expression for the point-spread function of the imaging algorithm is derived. The point-spread function (PDF) characterizes the resolution of the image, which is a function of the receiving array length and the ambient noise bandwidth. Results of a Monte Carlo simulation are presented to illustrate the theory.

Index Terms—Acoustic imaging, acoustic tomography, geophysical inverse problems, geophysical signal processing, geophysical tomography, image reconstruction, seismic inverse problems.

I. INTRODUCTION

IN time-exposure photography, low intensity light is integrated over time to enhance image brightness. A similar concept is applicable in acoustics, wherein acoustic or seismic imaging is performed using ambient acoustic noise as a constant source of “illumination.” The idea of passive acoustic imaging was recently demonstrated in an ocean environment by Buckingham and collaborators, in which submerged scatterers were imaged using ambient acoustic noise generated by surface wave action [1]–[3]. The authors refer to this method as “acoustic daylight imaging.” We propose extending the concept to seismic imaging of subsurface scatterers, including natural and man-made underground structures. Sources of ambient seismic noise are microseisms and surface noise due to weather and human activity.

Ambient imaging is potentially attractive since it avoids the high cost of the deployment and operation of active seismic sources. Moreover, ambient illumination is everpresent, thus permitting the “integration” of ambient data over an extended time period. In this way, relatively weak scatterers should eventually reveal themselves after a sufficient accumulation of data.

The basis of an imaging method using ambient illumination can be explained as follows. Seismic or acoustic waves impinging on a scatterer will create a scattered wavefront that will manifest itself as a spatially correlated signal over a receiving array on the surface. By coherently summing this correlated signal using a suitable migration (or backpropagation) procedure, the image of a weak scatterer should grow stronger over time relative to the uncorrelated background noise. One can conceive of devising an imaging algorithm that develops an image of the target as new data are incorporated into the image in a

recursive manner. In this way, storage of large quantities of data prior to forming the image can be avoided.

In the seismic domain, a few previous attempts have been reported on passively detecting large reflecting structures (e.g., a bedrock interface) [4]–[7]. As far as we are aware, however, no attempts have been made to image scatterers or diffracting structures (i.e., structures comparable to the wavelength of the illuminating waves) using ambient illumination. A more complete review of published work on passive seismic methods can be found in a recent report from the Oak Ridge National Laboratory, Oak Ridge, TN, [8] that presents results of a preliminary study on the feasibility of subsurface ambient imaging. In that study, no imaging was attempted using real data, but some important facts were established. First, ambient noise in the appropriate frequency range (up to 100 to 200 Hz) has adequate energy to be used for subsurface imaging, and second, cross-correlation of noise recorded by geophones in a two-dimensional (2-D) array showed peaks that relate to seismic energy propagating across the array. It was determined that the source of this spatially-coherent energy was traffic from a nearby road. An implication of the report is that the ability to suppress surface wave energy by digital filtering or optimal array design is critically important in separating ground roll from the upward propagating body waves scattered from subsurface structures.

An essential difference between active and ambient illumination is that, in the latter case, no time origin exists with respect to which propagation delays can be referenced. The illumination is effectively continuous and random. A greatly simplified analysis is possible if the illuminating waves can be regarded as spatially incoherent. Spatial incoherence is an idealization implying that the wave fields scattered from two distinct points in space are statistically uncorrelated over time. If waves are arriving from one direction from a distant and localized source, the assumption of spatially-incoherent illumination will break down. However, if the source of noise is primarily from the surface, which is generally the case at higher frequencies, then the assumption of spatial incoherence is probably quite good when the averaging is performed over an extended time period. It can be shown that the spatial resolution in an image derived from ambient noise is determined essentially by two factors: the length of the geophone array and the spatial coherence length of the noise. The latter is approximately the speed of sound divided by the noise bandwidth. For analytical tractability, we assume scatterers embedded in a background of constant velocity. Although the uniform background assumption is somewhat artificial, our primary aim in this paper is to investigate the resolution limits of a passive imaging scheme and relate it to the statistical properties of the seismic noise.

Below, an expression for the point-spread function (PSF, which is the image of a point scatterer) of an ambient imaging

Manuscript received March 31, 1999; revised December 16, 1999.

The authors are with Geophex, Ltd., Raleigh, NC 27603 USA (e-mail: norton@geophex.com).

Publisher Item Identifier S 0196-2892(00)03925-5.

system is derived assuming complete spatial incoherence of the noise. Suppose that $p(\mathbf{r}_1; t_1)$ and $p(\mathbf{r}_2; t_2)$ are signals scattered from the point \mathbf{r}_1 , and \mathbf{r}_2 . Then, complete spatial incoherence can be expressed as

$$E[p(\mathbf{r}_1; t_1)p(\mathbf{r}_2; t_2)^*] = P(t_1 - t_2)\delta(\mathbf{r}_1 - \mathbf{r}_2) \quad (1)$$

where $E[\cdot]$ denotes statistical expectation (i.e., an ensemble average), $\delta(\mathbf{r}_1 - \mathbf{r}_2)$ is a three-dimensional (3-D) Dirac delta function, and $P(\tau)$ is the temporal autocorrelation function of the noise. Here, we assume a stationary random process, implying that the argument of $P(\tau)$ is a function of the time difference $\tau = t_1 - t_2$. In (1), * denotes complex conjugate, since we reserve the option of working with analytic signals. We should point out that the relation (1) makes sense for a spatially incoherent source, but for a scattering problem, (1) will always represent an approximation whenever the autocorrelation function $P(\tau)$ has some finite duration (i.e., when the noise is bandlimited). This is because an incident waveform that is correlated over a finite time (given by the reciprocal of its bandwidth) will give rise to scattering that is spatially correlated over distances up to the spatial correlation length of the noise, given by c/B , where B is the bandwidth of the noise, and c is the speed of sound. As a consequence, the Dirac delta function in (1) will be broadened by this amount. If we consider scatterers farther apart than c/B , then the relation (1) effectively holds. In an imaging algorithm, it thus makes sense to make our pixel size larger than this correlation length. Image resolution can also be improved to some extent by applying a prewhitening filter to the received signals prior to image formation. Such a filter can help flatten the spectral response over the available bandwidth which, in the spatial domain, translates into a narrow point response.

The assumption of complete incoherence, expressed by (1), considerably simplifies the derivation of an analytical expression for the PSF. Later, we compare the analytically derived PSF to a more realistic computation of the PSF based on a Monte Carlo simulation of bandlimited stochastic noise using a random number generator. We shall see that the Monte Carlo simulation shows good agreement with the analytically derived PSF. The simulated images of several scatterers were obtained for various numbers of exposures, where each "exposure" refers to one image realization generated from one set of independent data. "Independent data" means that the interval of time separating data sets is taken to be greater than the reciprocal of the bandwidth of the noise. Assuming a bandwidth extending to 200 Hz, this implies an exposure interval of 0.005 s. Thus, 100 000 exposures would take no shorter than about 500 seconds of recording time. We will see that, as the number of exposures that are averaged increases, a gradual reduction in the uncorrelated background noise in the image is evident as data are continuously incorporated.

In the analysis that follows, we make several idealizing assumptions for the sake of analytical tractability, such as the assumption that stochastic scattering can be modeled as a weighted superposition of incoherent sources, and that multiple scattering is sufficiently small to neglect. It is likely, however, that the success of the method will not rest crucially on any of these idealizations, although performance may depart

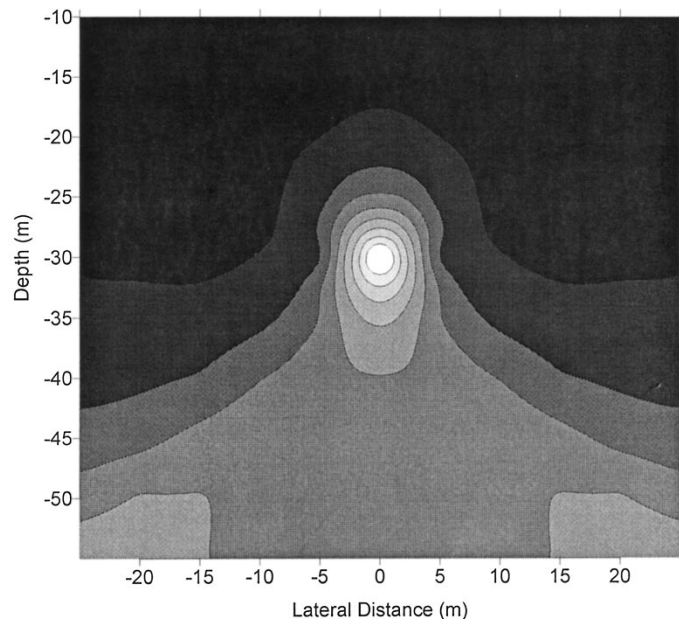


Fig. 1. Point-spread function (PSF) for a scatterer at a depth of 30 m, computed using (16) with surface data only.

somewhat from the results predicted by the analysis based on our simplifying assumptions.

II. IMAGING ALGORITHM

We model the earth as a distribution of scatterers of varying strengths (scattering cross-sections) embedded in a uniform background of constant velocity c . The extension to the case of nonuniform velocity can be made, provided that velocity information can be derived by independent means. We assume that the scattering medium is illuminated with broadband, spatially-incoherent noise. The noise is then passively recorded on the surface of the earth at N measurement points over some interval of time. Our objective is to reconstruct, or image, the scattering density distribution by backpropagating (migrating) the recorded noise into the earth. Because the source of illumination is always "turned on," an image of the scattering distribution can be gradually improved over time by recursively incorporating new data. The imaging algorithm coherently sums over the wavefront scattered from a point in the earth (equivalent to coherently summing along a hyperbolic path in the space-time domain) and assigns this value to the corresponding image point. This process is repeated for all image points until an entire image is generated. Multiple images created over successive time intervals are then added on an intensity basis as described below. As more data are incorporated, simulations show that the stochastic variability in the (mean) image due to the random nature of the illumination gradually diminishes, and weak scattering features become more apparent. After a certain large number of iterations, the image ceases to improve since all image noise has effectively been averaged out. Any remaining artifacts (e.g., the finite PSF width and sidelobe structure) are due to the inherent resolution limits of the system imposed by finite aperture and bandwidth constraints.

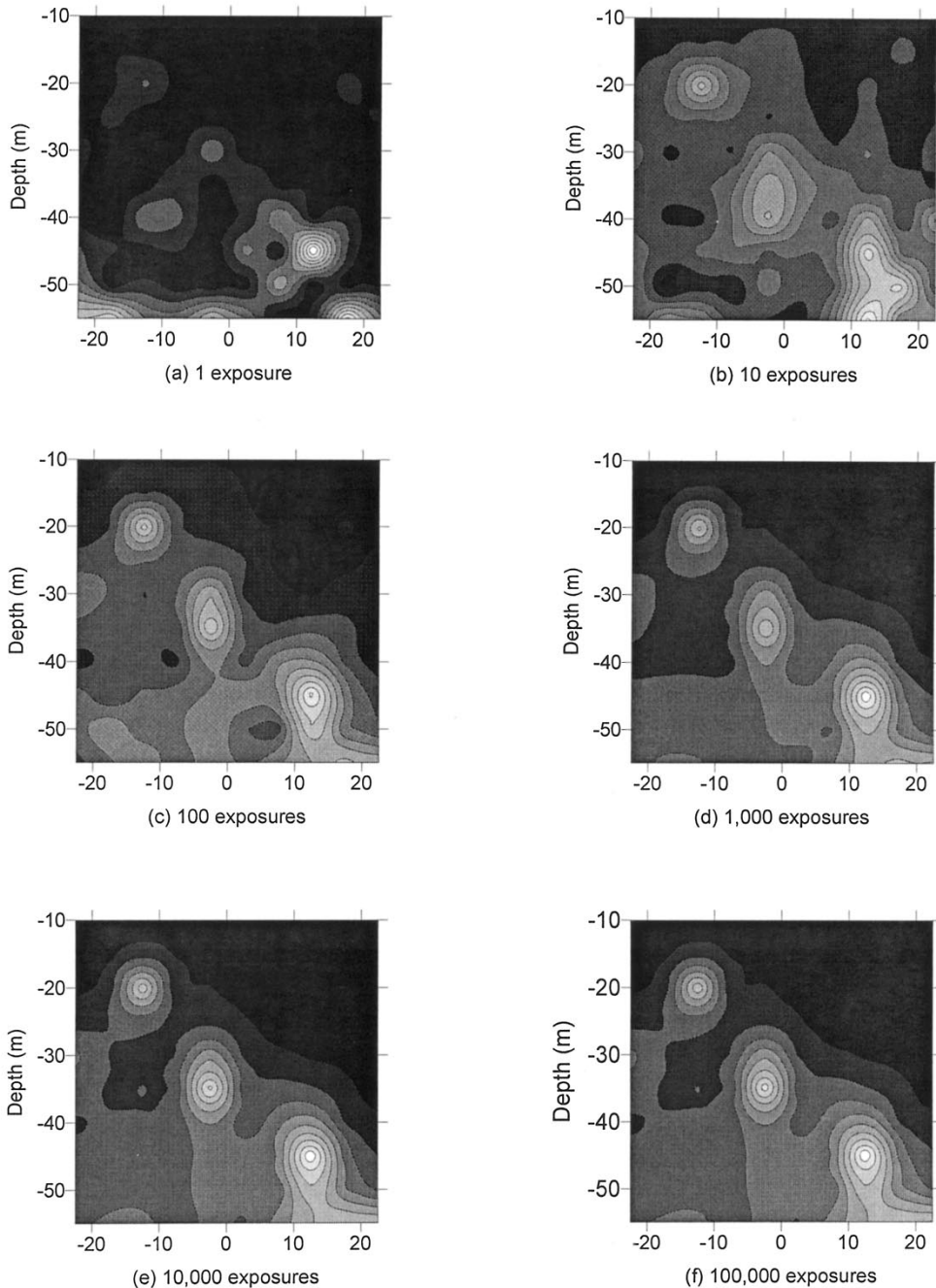


Fig. 2. Normalized images of three scatterers using stochastic data for different numbers of exposures with surface data only.

Below, we describe the imaging algorithm and derive from it the PSF of the system, which may be defined as the image of a single point scatterer. The PSF characterizes the lateral and depth resolution of the imaging system.

Let $u(\mathbf{r}_n, t)$ denote the field recorded at the point \mathbf{r}_n on the Earth's surface. Then the image generated by the process of backpropagation is given by

$$\mathcal{O}(\mathbf{r}) = 4\pi \sum_{n=1}^N \hat{u}(\mathbf{r}_n, |\mathbf{r} - \mathbf{r}_n|/c) |\mathbf{r} - \mathbf{r}_n| \quad (2)$$

where $\hat{u}(\mathbf{r}_n, t)$ is a filtered version of $u(\mathbf{r}_n, t)$. That is

$$\hat{u}(\mathbf{r}_n, t) = u(\mathbf{r}_n, t) * F(t) \quad (3)$$

with $*$ denoting convolution and $F(t)$ a specified filter function. For example, $F(t)$ could be a whitening filter. In (2), the factor $4\pi|\mathbf{r} - \mathbf{r}_n|$ is included to compensate for signal loss due to geometric spreading of the wave originating from the point \mathbf{r} .

For brevity, define $\hat{u}_n(\mathbf{r}) = 4\pi\hat{u}(\mathbf{r}_n, |\mathbf{r} - \mathbf{r}_n|/c) |\mathbf{r} - \mathbf{r}_n|$ so that (2) may be written

$$\mathcal{O}(\mathbf{r}) = \sum_{n=1}^N \hat{u}_n(\mathbf{r}). \quad (4)$$

The noise field $\hat{u}_n(\mathbf{r})$ is a random variable with zero mean. Letting $E\{\cdot\}$ denote statistical expectation (or ensemble average), we see that $E\{\mathcal{O}(\mathbf{r})\} = 0$, since the image $\mathcal{O}(\mathbf{r})$ is linear in the field $u(\mathbf{r}, t)$. This precludes averaging the images on an ‘‘amplitude’’ basis. We therefore consider averaging successive images on an intensity basis (i.e., averaging $|\mathcal{O}(\mathbf{r})|^2$). This, however, leads to a large DC bias in the image that builds up over time. An unbiased image estimator is obtained by subtracting the DC component as follows:

$$\bar{\mathcal{O}}(\mathbf{r}) = E \left\{ \left| \sum_{n=1}^N \hat{u}_n(\mathbf{r}) \right|^2 \right\} - E \left\{ \sum_{n=1}^N |\hat{u}_n(\mathbf{r})|^2 \right\} \quad (5)$$

which can also be written

$$\bar{\mathcal{O}}(\mathbf{r}) = \sum_{n=1}^N \sum_{\substack{m=1 \\ n \neq m}}^N E\{\hat{u}_n(\mathbf{r})\hat{u}_m(\mathbf{r})^*\}. \quad (6)$$

Equation (6) shows that if there is no correlation between distinct traces $\hat{u}_n(\mathbf{r})$, then the image $\bar{\mathcal{O}}(\mathbf{r})$ vanishes as desired. Otherwise, it is positive. The first term in (5) bears some resemblance to the coherence measure called the semblance [9].

Suppose we denote by $\mathcal{O}^{(k)}(\mathbf{r})$ the k th image realization. We wish to average many such realizations to approximate the ensemble average indicated by the expectation operator $E\{\cdot\}$ in (5). That is, the average of M images is

$$\bar{\mathcal{O}}_M(\mathbf{r}) = \frac{1}{M} \sum_{k=1}^M \mathcal{O}^{(k)}(\mathbf{r}) \quad (7)$$

where the k th realization is defined by

$$\mathcal{O}^{(k)}(\mathbf{r}) = \left| \sum_{n=1}^N \hat{u}_n^{(k)}(\mathbf{r}) \right|^2 - \sum_{n=1}^N |\hat{u}_n^{(k)}(\mathbf{r})|^2. \quad (8)$$

To avoid storing large amounts of data, one can update the average (7) recursively as more data become available. Given the average $\bar{\mathcal{O}}_M(\mathbf{r})$ formed after M image realizations, the updated average $\bar{\mathcal{O}}_{M+1}(\mathbf{r})$ after the $M+1$ realization $\mathcal{O}^{(M+1)}(\mathbf{r})$ becomes available is

$$\bar{\mathcal{O}}_{M+1}(\mathbf{r}) = \frac{M}{M+1} \bar{\mathcal{O}}_M(\mathbf{r}) + \frac{1}{M+1} \mathcal{O}^{(M+1)}(\mathbf{r}). \quad (9)$$

III. DERIVATION OF SYSTEM POINT SPREAD FUNCTION

Below, we derive an analytical form for the PSF. Our basic objective is to evaluate analytically the first term in (5), which represents the actual image. The purpose of the second term is essentially to eliminate a DC bias, or constant background, from this image. For analytical tractability, we assume that the receiving array is continuously sampled, in which case, the sum over n in (5) becomes an integral over the array aperture. We model the medium as a continuum of scatterers embedded in a background of constant velocity c . The density of scatterers at the point \mathbf{r} is denoted by $\sigma(\mathbf{r})$. That is, $\sigma(\mathbf{r})$ can be regarded as a continuously varying scattering cross-section, and our objective

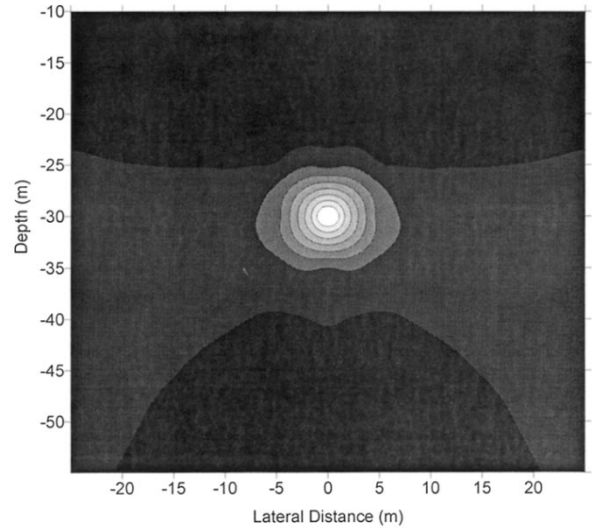


Fig. 3. PSF for a scatterer computed using (16), assuming both surface and borehole data.

is to reconstruct $\sigma(\mathbf{r})$. Suppose random noise is illuminating the medium from many directions, and let $p(\mathbf{r}; t)$ denote the noise scattered from the point \mathbf{r} . Then the signal received at a point \mathbf{r}_a on the array may be written as the following integral over the medium

$$u(\mathbf{r}_a, t) = \iiint \sigma(\mathbf{r}') \frac{p[\mathbf{r}'; t - |\mathbf{r}' - \mathbf{r}_a|/c]}{4\pi|\mathbf{r}' - \mathbf{r}_a|} d^3\mathbf{r}'. \quad (10)$$

In this simple model, multiple scattering has been neglected. For a 3-D reconstruction, we record data over a 2-D array on the surface of the earth. Letting \mathbf{r}_a represent a point on this array and A the region of the surface occupied by the array, then the backpropagation operation can be expressed as follows, where, for generality, we again allow filtering prior to backpropagation:

$$\mathcal{O}(\mathbf{r}) = 4\pi \iint_A d^2\mathbf{r}_a \hat{u}(\mathbf{r}_a, |\mathbf{r} - \mathbf{r}_a|/c) |\mathbf{r} - \mathbf{r}_a| \quad (11)$$

which is the continuous space analogue of (2). Once again, $\hat{u}(\mathbf{r}_a, t)$ is a filtered version of the recorded data $u(\mathbf{r}_a, t)$, i.e.,

$$\hat{u}(\mathbf{r}_a, t) = u(\mathbf{r}_a, t) * F(t) \quad (12)$$

for a specified filter function $F(t)$.

To compute the image, we substitute (10) into (11) and interchange orders of integration. This gives

$$\mathcal{O}(\mathbf{r}) = \iiint d^3\mathbf{r}' \sigma(\mathbf{r}') \iint_A d^2\mathbf{r}_a \cdot \frac{|\mathbf{r} - \mathbf{r}_a|}{|\mathbf{r}' - \mathbf{r}_a|} \hat{p}[\mathbf{r}'; |\mathbf{r} - \mathbf{r}_a|/c - |\mathbf{r}' - \mathbf{r}_a|/c] \quad (13)$$

where $\hat{p}(\mathbf{r}; t) = p(\mathbf{r}; t) * F(t)$. Now take the absolute square of (13), perform an ensemble average, and use the relation (1). This gives rise to the following result:

$$E[|\mathcal{O}(\mathbf{r})|^2] = \iiint d^3\mathbf{r}' \sigma(\mathbf{r}')^2 \text{PSF}(\mathbf{r}; \mathbf{r}') \quad (14)$$

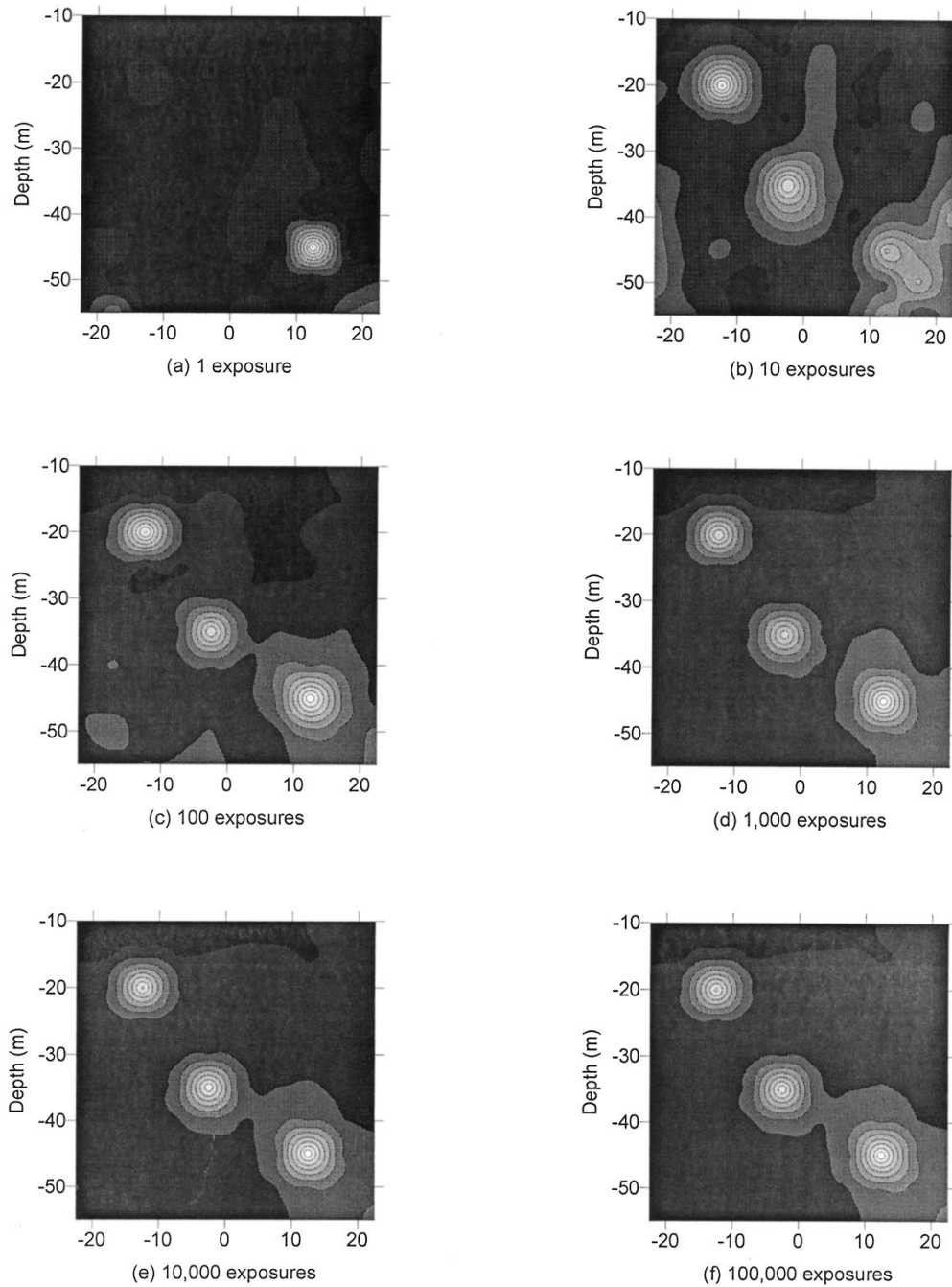


Fig. 4. Normalized images of three scatterers using stochastic data for different numbers of exposures assuming both surface and borehole data.

where $PSF(\mathbf{r}; \mathbf{r}')$ is the PSF defined by

$$PSF(\mathbf{r}; \mathbf{r}') \equiv \iint_A d^2\mathbf{r}_a \frac{|\mathbf{r} - \mathbf{r}_a|}{|\mathbf{r}' - \mathbf{r}_a|} \iint_A d^2\mathbf{r}'_a \cdot \frac{|\mathbf{r} - \mathbf{r}'_a|}{|\mathbf{r}' - \mathbf{r}'_a|} \hat{P}[(R_a - R'_a)/c] \quad (15)$$

with

$$R_a \equiv |\mathbf{r} - \mathbf{r}_a| - |\mathbf{r}' - \mathbf{r}_a|$$

$$R'_a \equiv |\mathbf{r} - \mathbf{r}'_a| - |\mathbf{r}' - \mathbf{r}'_a|.$$

In (15), $\hat{P}(\tau)$ is the filtered version of $P(\tau)$, i.e., $\hat{P}(\tau)$ is the autocorrelation function $E[\hat{p}(\mathbf{r}; t + \tau)\hat{p}^*(\mathbf{r}; t)]$.

We can simplify the above expression for the PSF as follows. Let $\tilde{P}(\omega)$ denote the Fourier transform of $P(t)$, that is

$$P(t) = \int_{-\infty}^{\infty} \tilde{P}(\omega) e^{i\omega t} d\omega.$$

Note that $\tilde{P}(\omega)$ is the noise power spectrum. Then

$$\tilde{P}(t) = \int_{-\infty}^{\infty} \tilde{P}(\omega) |\tilde{F}(\omega)|^2 e^{i\omega t} d\omega$$

where $\tilde{F}(\omega)$ is the Fourier transform of the filter function $F(t)$. Substituting this into (15) results in

$$\text{PSF}(\mathbf{r}; \mathbf{r}') = \int_{-\infty}^{\infty} d\omega \tilde{P}(\omega) |\tilde{F}(\omega)|^2 |A_\omega(\mathbf{r}; \mathbf{r}')|^2 \quad (16)$$

where

$$A_\omega(\mathbf{r}; \mathbf{r}') \equiv \iint_A d^2\mathbf{r}_a \frac{|\mathbf{r} - \mathbf{r}_a|}{|\mathbf{r}' - \mathbf{r}_a|} \cdot \exp[i\omega(|\mathbf{r} - \mathbf{r}_a| - |\mathbf{r}' - \mathbf{r}_a|)/c]. \quad (17)$$

Clearly, at each frequency ω , the function $A_\omega(\mathbf{r}; \mathbf{r}')$ will become large when the image point \mathbf{r} coincides with the scattering point \mathbf{r}' since then the exponent vanishes. In the next section, we show a numerical computation of the PSF using (16) and (17), and compare it to a Monte Carlo simulation.

IV. SIMULATIONS

Fig. 1 shows an image of PSF $\text{PSF}(\mathbf{r}; \mathbf{r}_0)$ obtained by numerically evaluating (16) and (17) over a linear array. In computing the PSF, the scattering point was placed at $\mathbf{r}' = (0, -30)$ in units of meters. Twenty receiving elements were assumed, spaced at 5-m intervals (implying an array length of 95 m). The power spectrum $\tilde{P}(\omega)$ was assumed, for simplicity, to extend uniformly to 200 Hz. A velocity of sound of 500 m/s was used. We note that if the velocity is scaled up and the noise bandwidth remains unchanged then the appearance of all images will remain unchanged, provided all distances are scaled in proportion to the velocity.

Fig. 2 shows the results of a Monte Carlo simulation using (7) and (8), which combine multiple image realizations, each generated by the backpropagation process defined by (2). In the simulation, three scatterers were assumed at coordinates $(-12.5, -20)$, $(-2.5, -35)$, and $(12.5, -45)$. We regarded each of these three points as behaving effectively as independent sources of broadband random noise. As noted, this is a reasonable model when the noise correlation distance is smaller than the scatterer separations. Finally, surface interactions and multiple scattering between the scatterers were neglected in the simulation.

The number of exposures indicated in Fig. 2 is defined as the number of terms M in the summation (7). In each image realization, backpropagation to a 10×10 array of pixels was performed with a center-to-center pixel separation of 5 m. The simulated scattered waveform $u(\mathbf{r}, t)$ was created using a random number generator to produce a zero-mean, uniformly distributed sequence of samples at a sampling interval of 0.0025 s, corresponding to a Nyquist rate of 200 Hz. This implies a noise correlation length c/B equal to 2.5 m when $B = 200$ Hz and $c = 500$ m/s. Thus, the center-to-center pixel spacing is greater than the correlation length. The numbers of exposures averaged are indicated in the figure. Each image has been normalized to unity to show clearly how background artifacts are reduced as the exposure number increases. In this particular simulation, the image

quality reaches a steady state above about 1000 exposures. This means that nearly all of the stochastic variability has been eliminated at this point, and the remaining artifacts (PSF broadening and sidelobe structure) are determined by the inherent bandwidth and aperture limitations of the system.

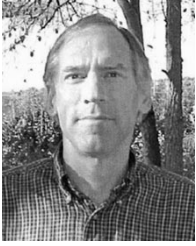
The above simulation assumed an array of 20 geophones on the surface of the earth. Another simulation was performed with both surface geophones and borehole geophones. The same scatterers, velocity, and noise bandwidth were assumed. In this case, however, 60 geophones were assumed in the simulation, 20 on the surface, 20 distributed vertically down a borehole to the left of the scattering region, and 20 in a borehole to the right of the scattering region. The three geophone array segments, one surface and two borehole, were assumed to be of the same length (95 m). The PSF for this array configuration was again computed using (16) and (17) and is shown in Fig. 3. Next, the results of a Monte Carlo simulation are shown in Fig. 4. Note that both the PSF and the simulated images are sharper and more symmetrical due to the extended system aperture created by the addition of the boreholes data.

V. CONCLUSION

A theoretical investigation of the possibility of imaging underground scatterers employing ambient illumination was presented. For simplicity, we assumed that the scatterers were embedded in a constant velocity background, but the extension to nonuniform velocity is expected to yield qualitatively similar results. Under the assumption of spatially incoherent noise, an analytical expression for the PSF was derived. This expression characterizes both transverse and depth resolution and defines their dependence on array length and the ambient noise bandwidth. Monte Carlo simulations were performed to demonstrate that multiple exposures, added together as data are continuously acquired, will diminish uncorrelated background noise and improve image quality.

REFERENCES

- [1] M. J. Buckingham, B. V. Berkhout, and S. A. Glegg, "Imaging the ocean with ambient noise," *Nature*, vol. 356, pp. 327–329, 1992.
- [2] M. J. Buckingham, "Theory of acoustic imaging in the ocean with ambient noise," *J. Comput. Acoust.*, vol. 1, pp. 117–140, 1993.
- [3] J. R. Potter, "Acoustic imaging using ambient noise: Some theory and simulation results," *J. Acoust. Soc. Amer.*, vol. 95, pp. 21–33, 1994.
- [4] L. J. Katz, "Microtremor analysis of local geologic conditions," *Bull. Seis. Soc. Amer.*, vol. 66, pp. 45–60, 1985.
- [5] —, "Passive seismic groundnoise: A novel approach to exploration, Extended abstract," in *Proc. 55th Annu. Int. Meeting Society Exploration Geophysicists*, Washington, DC, 1989, pp. 181–183.
- [6] S. P. Cole, "Passive seismic and drill-bit experiments using 2-D arrays," Ph.D. thesis, Stanford University, Stanford, CA, 1996.
- [7] S. P. Cole, J. F. Claerbout, D. E. Nichols, and L. Zhang, "The ambient seismic field in three dimensions," submitted for publication.
- [8] W. E. Doll, S. J. Norton, L. J. Gray, and M. D. Morris, "Passive seismic imaging of scatterers," Oak Ridge National Lab., Oak Ridge, TN, Tech. Rep. K/NSP-585, Oct. 1997.
- [9] N. S. Neidell and M. T. Taner, "Semblance and other coherency measures for multichannel data," *Geophys.*, vol. 36, pp. 482–497, 1971.
- [10] J. W. Goodman, *Fourier Optics*. New York: McGraw-Hill, 1968.



Stephen J. Norton received the B.A. in physics from the University of California, Berkeley, in 1971, and the Ph.D. in applied physics from Stanford University, Stanford, CA, in 1976.

He was a National Research Council (NRC) Postdoctoral Fellow with the National Bureau of Standards from 1977 to 1979, and worked in the fields of medical imaging and the nondestructive evaluation of materials at the National Institute of Standards and Technology, Gaithersburg, MD, from 1979 to 1993. He then spent five years at the Oak Ridge National

Laboratory working in the area of geophysical imaging before joining Geophex, Ltd., Raleigh, NC, in 1998. He has published about 75 papers on all aspects of inversion and imaging, including diffraction tomography, magnetic resonance imaging, Mossbauer tomography, ultrasonic imaging in medicine and NDE, Compton scattering tomography, and electromagnetic induction imaging.



I. J. Won received the B.S. degree in mining and petroleum engineering in 1967 from Seoul National University, Seoul, Korea, and the M.S. and Ph.D. degrees in geophysics from Columbia University, New York, in 1971 and 1973, respectively.

He is currently Technical Director and President of Geophex, Ltd., an independent geological and environmental consulting firm based in Raleigh, NC, which he founded in 1983. From 1976 until 1989, he was an Assistant Professor, Associate Professor, and Professor of Geophysics with North Carolina State

University, Raleigh. He has published over 70 research and review articles in refereed technical journals and books. He specializes in geophysical applications to geotechnical and environmental problems.